US011146232B2

(12) **United States Patent**
Yandrapalli et al.

(10) **Patent No.: US 11,146,232 B2**
(45) **Date of Patent: Oct. 12, 2021**

(54) **TRANSVERSELY-EXCITED FILM BULK ACOUSTIC RESONATOR WITH REDUCED SPURIOUS MODES**

(71) Applicant: **Resonant Inc.**, Goleta, CA (US)

(72) Inventors: **Soumya Yandrapalli**, Lausanne (CH); **Viktor Plesski**, Gorgier (CH); **Julius Koskela**, Helsinki (FI); **Ventsislav Yantchev**, Sofia (BG); **Patrick Turner**, San Bruno, CA (US)

(73) Assignee: **Resonant Inc.**, Austin, TX (US)

(*) Notice: Subject to any disclaimer, the term of this patent is extended or adjusted under 35 U.S.C. 154(b) by 79 days.

(21) Appl. No.: **17/030,066**

(22) Filed: **Sep. 23, 2020**

(65) **Prior Publication Data**

US 2021/0028757 A1 Jan. 28, 2021

Related U.S. Application Data

(63) Continuation-in-part of application No. 16/920,173, filed on Jul. 2, 2020, which is a continuation of
(Continued)

(51) **Int. Cl.**
H03H 9/02 (2006.01)
H03H 3/04 (2006.01)
(Continued)

(52) **U.S. Cl.**
CPC ***H03H 9/02228*** (2013.01); ***H03H 3/04*** (2013.01); ***H03H 9/02031*** (2013.01);
(Continued)

(58) **Field of Classification Search**
CPC .. H03H 9/02228; H03H 3/04; H03H 9/02031; H03H 9/132; H03H 9/174;
(Continued)

(56) **References Cited**

U.S. PATENT DOCUMENTS

5,552,655 A * 9/1996 Stokes H03H 9/02228 310/321
6,540,827 B1 4/2003 Levy et al.
(Continued)

FOREIGN PATENT DOCUMENTS

WO 2016017104 2/2016
WO 2018003273 A1 1/2018

OTHER PUBLICATIONS

Namdeo et al. "Simulation on Effects of Electrical Loading due to Interdigital Transducers in Surface Acoustic Wave Resonator", published in Procedia Engineering 64 (2013) of Science Direct pp. 322-330 (Year: 2013).*
(Continued)

Primary Examiner — Hafizur Rahman
(74) *Attorney, Agent, or Firm* — Socal IP Law Group LLP; John E. Gunther

(57) **ABSTRACT**

Acoustic filters, resonators and methods are disclosed. An acoustic resonator device includes a substrate having a surface. A back surface of a single-crystal piezoelectric plate is attached to the surface of the substrate except for a portion of the piezoelectric plate forming a diaphragm that spans a cavity in the substrate. A conductor pattern is formed on the front surface of the piezoelectric plate, the conductor pattern including an interdigital transducer (IDTs), interleaved fingers of the IDT disposed on the diaphragm. A pitch of the interleaved fingers and a mark of the interleaved fingers are set in combination such that a resonance frequency of the acoustic resonator is equal to a predetermined target frequency.

18 Claims, 11 Drawing Sheets

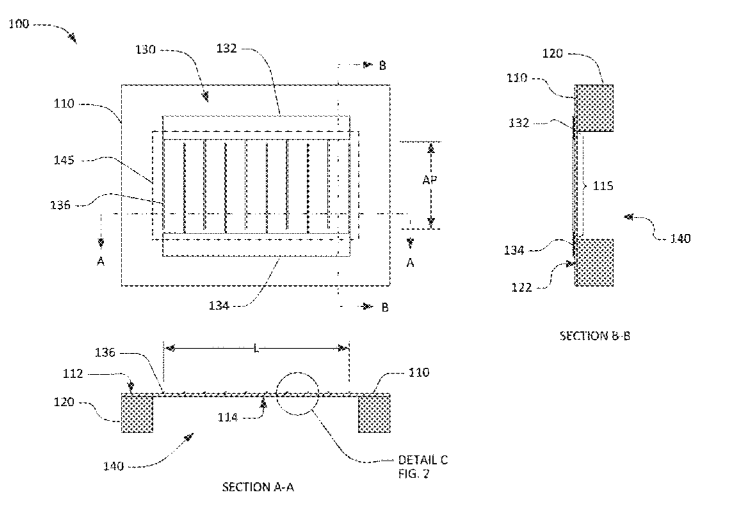

Related U.S. Application Data

application No. 16/438,121, filed on Jun. 11, 2019, now Pat. No. 10,756,697, which is a continuation-in-part of application No. 16/230,443, filed on Dec. 21, 2018, now Pat. No. 10,491,192.

(60) Provisional application No. 62/904,386, filed on Sep. 23, 2019, provisional application No. 62/753,815, filed on Oct. 31, 2018, provisional application No. 62/748,883, filed on Oct. 22, 2018, provisional application No. 62/741,702, filed on Oct. 5, 2018, provisional application No. 62/701,363, filed on Jul. 20, 2018, provisional application No. 62/685,825, filed on Jun. 15, 2018.

(51) **Int. Cl.**
H03H 9/13 (2006.01)
H03H 9/17 (2006.01)
H03H 9/56 (2006.01)
H03H 3/02 (2006.01)

(52) **U.S. Cl.**
CPC ***H03H 9/132*** (2013.01); ***H03H 9/174*** (2013.01); ***H03H 9/176*** (2013.01); ***H03H 9/562*** (2013.01); ***H03H 9/564*** (2013.01); ***H03H 9/568*** (2013.01); *H03H 2003/023* (2013.01); *H03H 2003/0442* (2013.01)

(58) **Field of Classification Search**
CPC H03H 9/176; H03H 9/562; H03H 9/564; H03H 9/568; H03H 2003/023; H03H 2003/0442
USPC 333/186, 187, 189
See application file for complete search history.

(56) **References Cited**

U.S. PATENT DOCUMENTS

7,463,118	B2	12/2008	Jacobsen	
7,535,152	B2	5/2009	Ogami et al.	
7,684,109	B2	3/2010	Godshalk et al.	
7,728,483	B2 *	6/2010	Tanaka	H03H 9/02023 310/313 R
7,868,519	B2	1/2011	Umeda	
8,278,802	B1	10/2012	Lee et al.	
8,829,766	B2	9/2014	Milyutin et al.	
8,932,686	B2	1/2015	Hayakawa et al.	
9,219,466	B2	12/2015	Meltaus et al.	
9,276,557	B1	3/2016	Nordquist et al.	
9,369,105	B1	6/2016	Li	
9,425,765	B2	8/2016	Rinaldi	
9,525,398	B1	12/2016	Olsson	
9,780,759	B2	10/2017	Kimura et al.	
2002/0158714	A1	10/2002	Kaitila et al.	
2004/0261250	A1	12/2004	Kadota et al.	
2005/0185026	A1 *	8/2005	Noguchi	C04B 35/499 347/68
2011/0109196	A1	5/2011	Goto	
2013/0234805	A1	9/2013	Takahashi	
2014/0145556	A1	5/2014	Kadota	
2014/0151151	A1	6/2014	Reinhardt	
2015/0319537	A1	11/2015	Perois et al.	
2015/0333730	A1	11/2015	Meltaus	
2016/0182009	A1	6/2016	Bhattacharjee	
2017/0063332	A1	3/2017	Gilbert et al.	
2017/0179928	A1	6/2017	Raihn et al.	
2017/0214387	A1	7/2017	Burak et al.	
2017/0222622	A1	8/2017	Solal et al.	
2019/0068164	A1	2/2019	Houlden et al.	
2019/0131953	A1	5/2019	Gong	
2019/0273480	A1	9/2019	Lin	

OTHER PUBLICATIONS

Rodríguez-Madrid et al., "Super-High-Frequency SAW Resonators on AIN/Diamond", IEEE Electron Device Letters, vol. 33, No. 4, Apr. 2012, pp. 495-497. (Year: 2012).*

Santosh G, Surface acoustic wave devices on silicon using patterned and thin film ZnO, Ph.D. thesis, Indian Institute of technology Guwahati, Assam, India, Feb. 2016, p. 50 added (Year: 2016).*

T. Takai, H. Iwamoto, et al., "I.H.P.Saw Technology and its Application to Microacoustic Components (Invited)." 2017 IEEE International Ultrasonics Symposium, Sep. 6-9, 2017. pp. 1-8.

R. Olsson III, K. Hattar et al. "A high electromechanical coupling coefficient SH0 Lamb wave lithiumniobate micromechanical resonator and a method for fabrication" Sensors and Actuators A: Physical, vol. 209, Mar. 1, 2014, pp. 183-190.

M. Kadota, S. Tanaka, "Wideband acoustic wave resonators composed of hetero acoustic layer structure," Japanese Journal of Applied Physics, vol. 57, No. 7S1. Published Jun. 5, 2018. 5 pages.

Y. Yang, R. Lu et al. "Towards Ka Band Acoustics: Lithium Niobat Asymmetrical Mode Piezoelectric MEMS Resonators", Department of Electrical and Computer Engineering University of Illinois at Urbana-Champaign, May 2018. pp. 1-2.

Y. Yang, A. Gao et al. "5 GHz Lithium Niobate MEMS Resonators With High FOM of 153", 2017 IEEE 30th International Conference in Micro Electro Mechanical Systems (MEMS). Jan. 22-26, 2017. pp. 942-945.

USPTO/ISA, International Search Report and Written Opinion for PCT Application No. PCT/US2019/036433 dated Aug. 29, 2019.

USPTO/ISA, International Search Report and Written Opinion for PCT Application No. PCT/US2019/058632 dated Jan. 17, 2020.

G. Manohar, "Investigation of Various Surface Acoustic Wave Design Configurations for Improved Sensitivity." Doctoral dissertation, University of South Florida, USA, Jan. 2012, 7 pages.

Ekeom, D. & Dubus, Bertrand & Volatier, A.. (2006). Solidly mounted resonator (SMR) FEM-BEM simulation. 1474-1477. 10.1109/ULTSYM.2006.371.

Mizutaui, K. and Toda, K., "Analysis of lamb wave propagation characteristics in rotated Y-cut X-propagation LiNbO3 plates." Electron. Comm. Jpn. Pt. I, 69, No. 4 (1986): 47-55. doi:10.1002/ecja.4410690406.

Naumenko et al., "Optimal orientations of Lithium Niobate for resonator SAW filters", 2003 IEEE Ultrasonics Symposium—pp. 2110-2113. (Year: 2003).

* cited by examiner

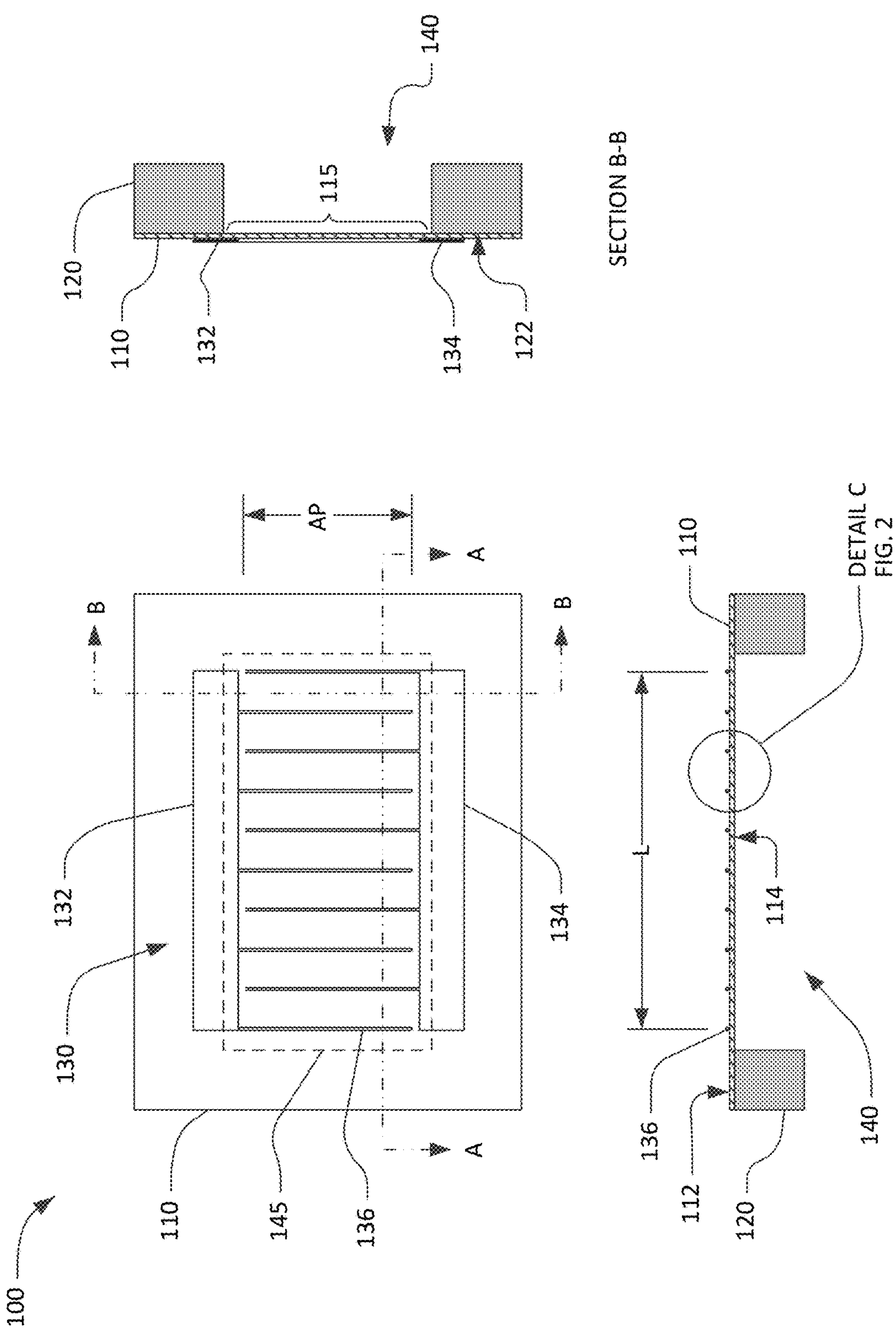
100
110
130
132
134
136
145
AP
A
B
L
114
112
120
140
DETAIL C
FIG. 2
SECTION A-A
SECTION B-B
115
122

FIG. 1

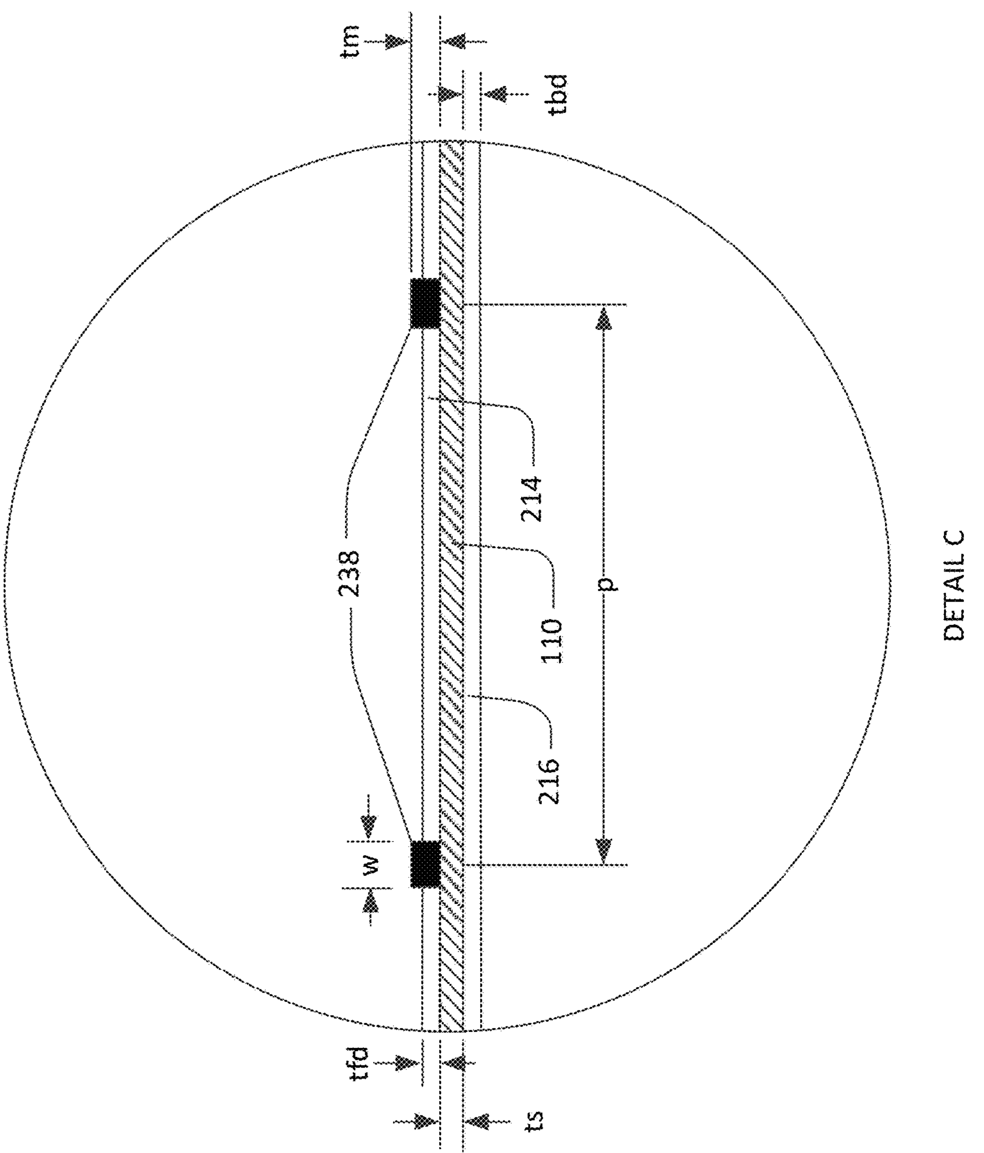

FIG. 2

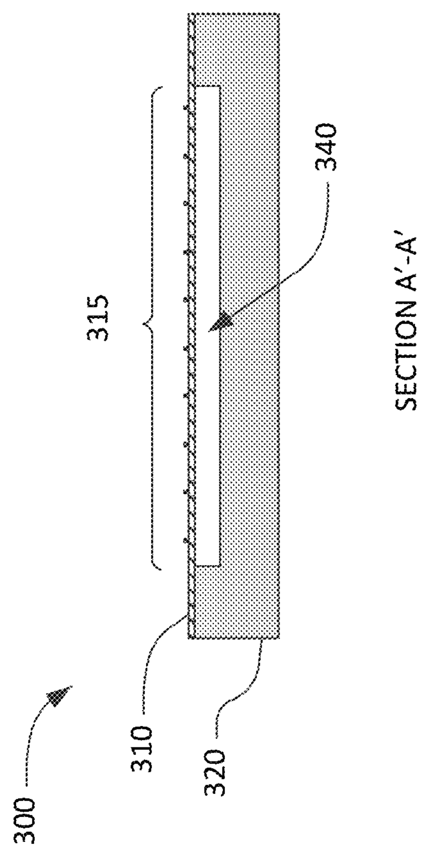

FIG. 3

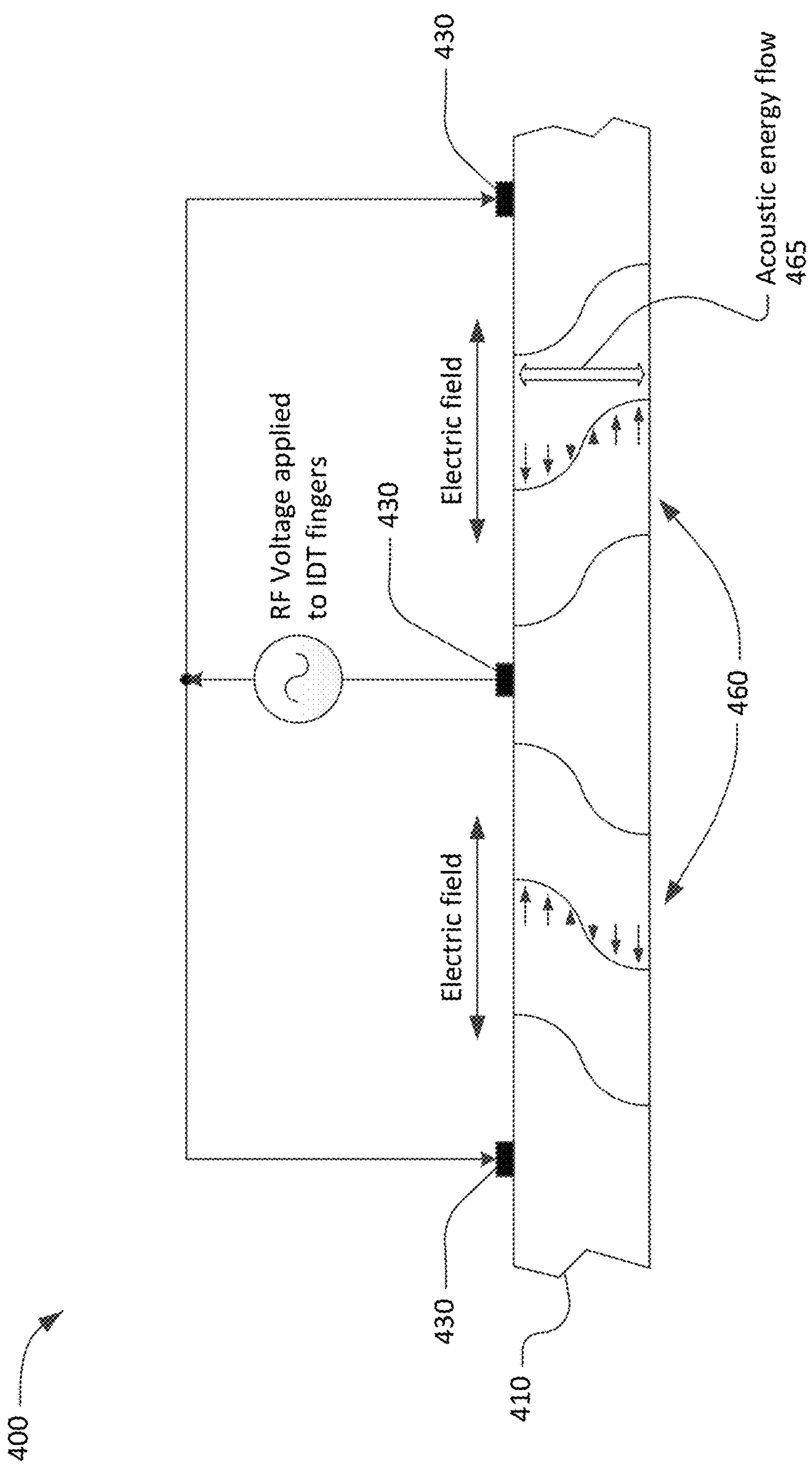
400
410
430
430
430
RF Voltage applied
to IDT fingers
Electric field
Electric field
460
Acoustic energy flow
465

FIG. 4

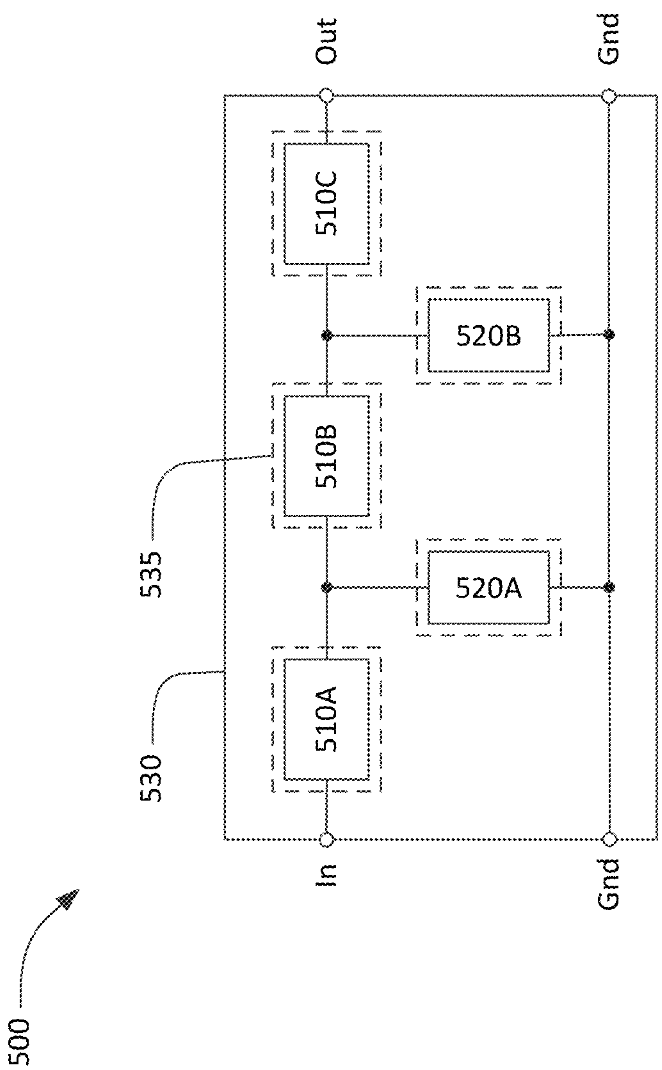

FIG. 5

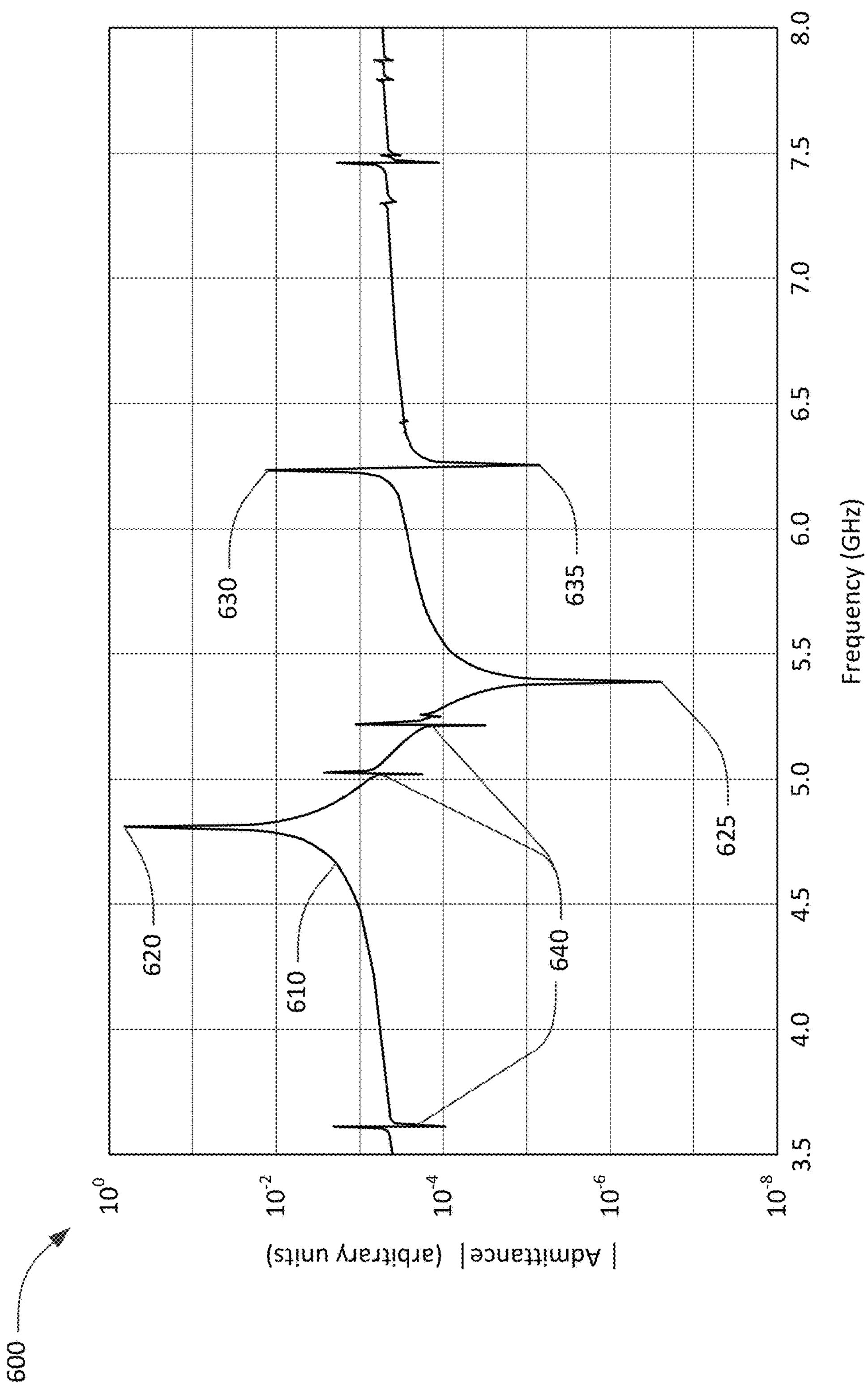
600
| Admittance | (arbitrary units)
10^0
10^-2
10^-4
10^-6
10^-8
Frequency (GHz)
3.5
4.0
4.5
5.0
5.5
6.0
6.5
7.0
7.5
8.0
620
610
640
625
630
635

FIG. 6

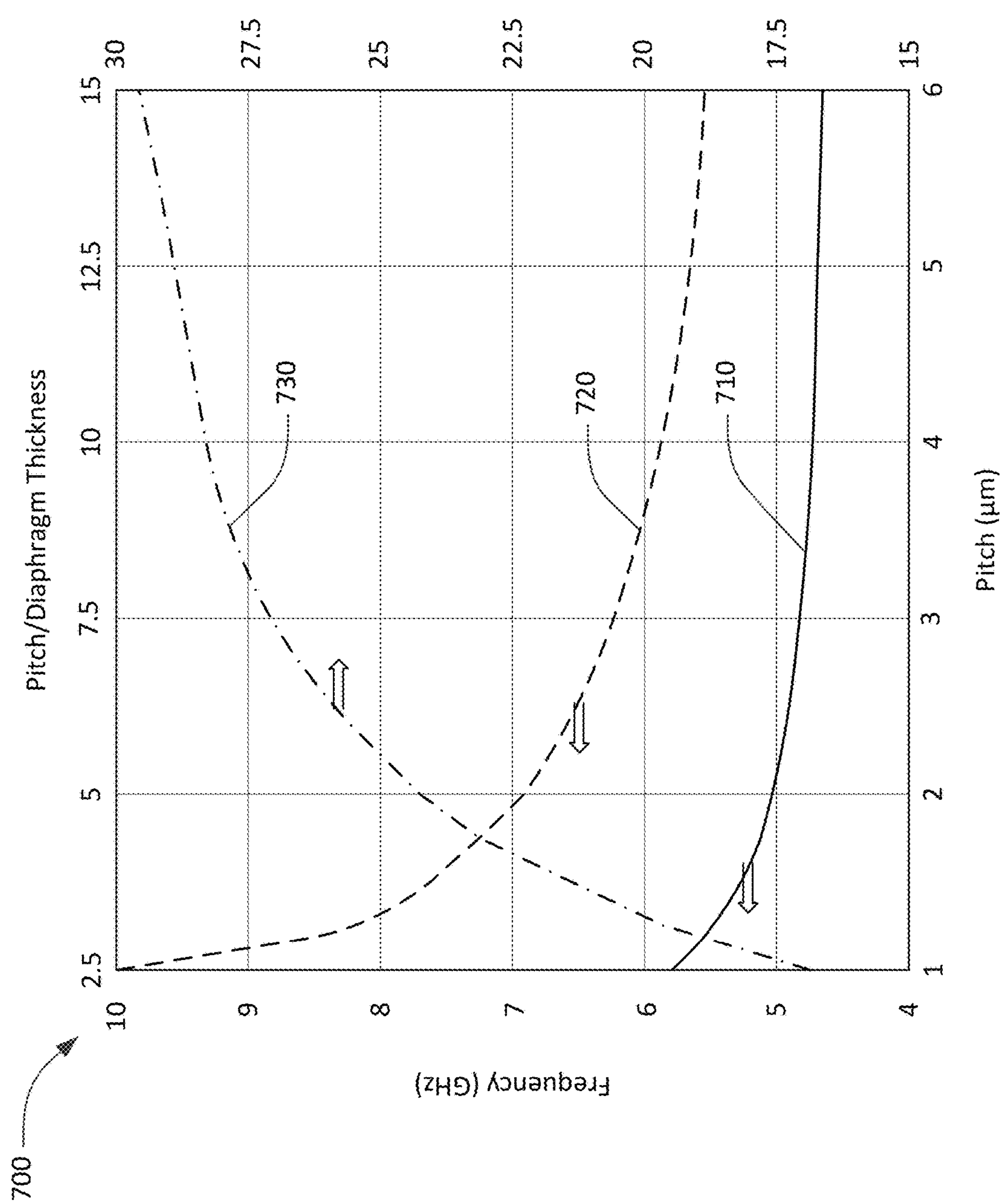
700
Pitch/Diaphragm Thickness
Coupling (%)
Frequency (GHz)
Pitch (µm)
710
720
730
2.5
5
7.5
10
12.5
15
30
27.5
25
22.5
20
17.5
15
10
9
8
7
6
5
4
1
2
3
4
5
6

FIG. 7

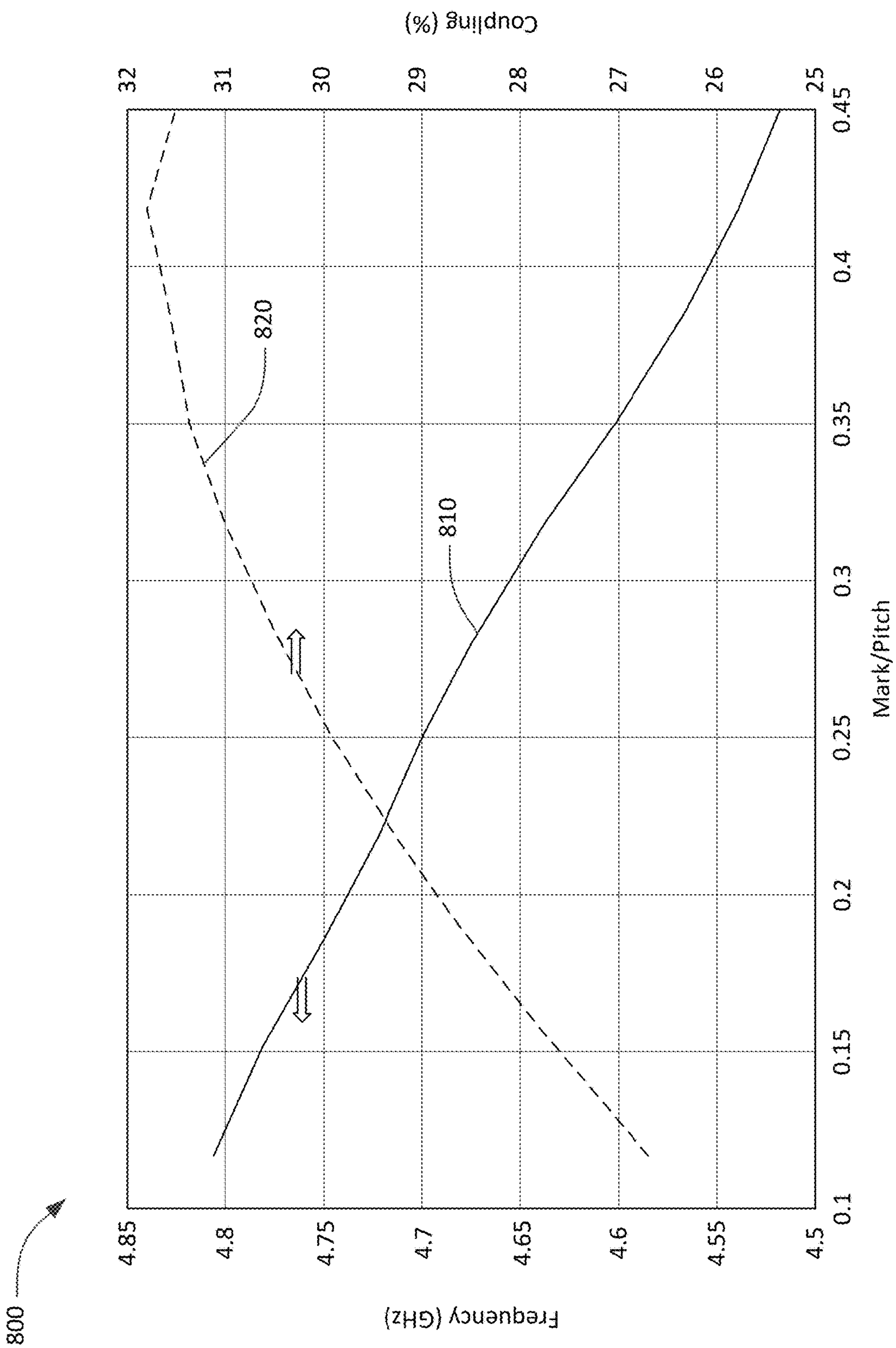
800
Frequency (GHz)
4.85
4.8
4.75
4.7
4.65
4.6
4.55
4.5
Coupling (%)
32
31
30
29
28
27
26
25
0.1
0.15
0.2
0.25
0.3
0.35
0.4
0.45
Mark/Pitch
810
820

FIG. 8

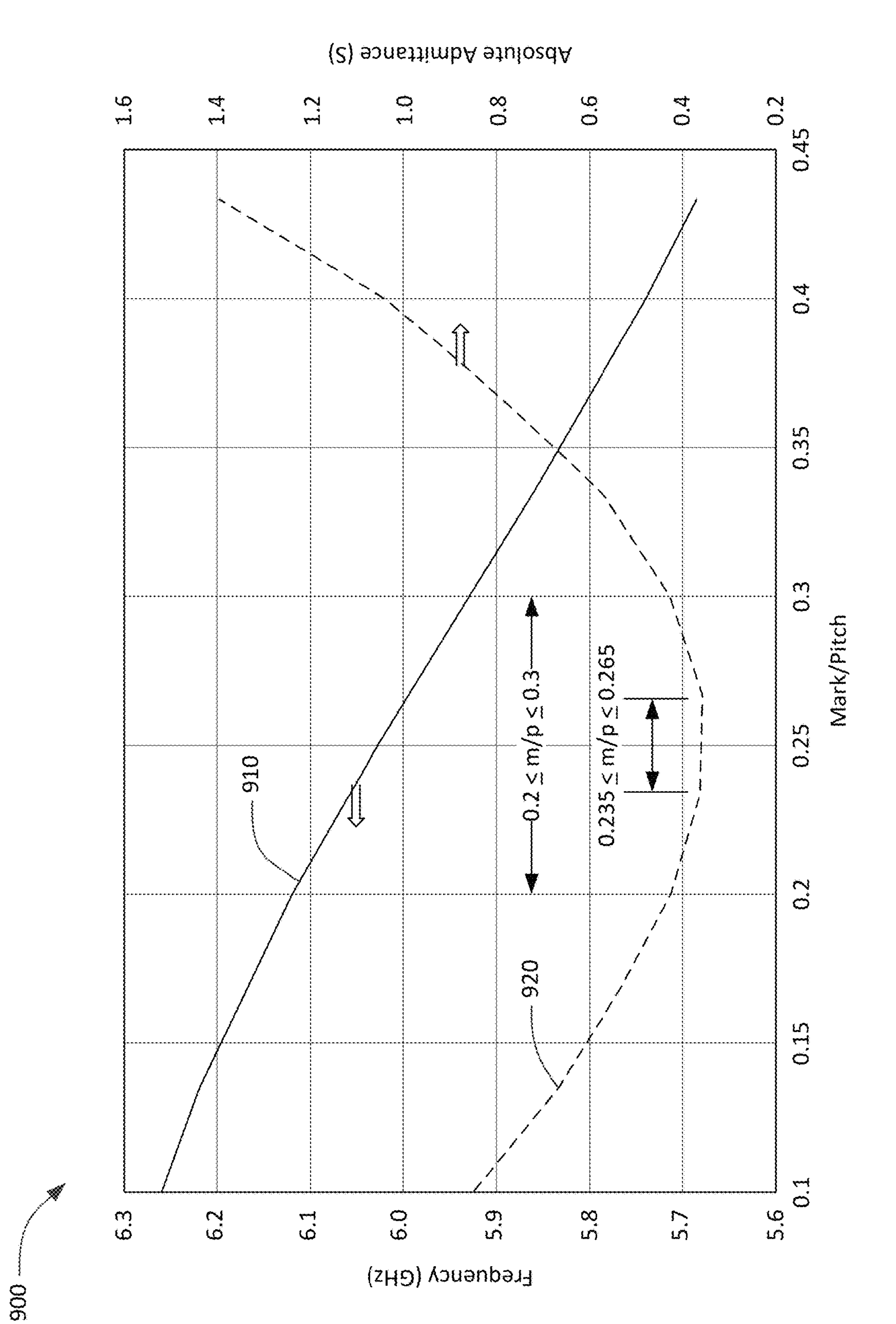
900
Frequency (GHz)
6.3
6.2
6.1
6.0
5.9
5.8
5.7
5.6
Absolute Admittance (S)
1.6
1.4
1.2
1.0
0.8
0.6
0.4
0.2
Mark/Pitch
0.1
0.15
0.2
0.25
0.3
0.35
0.4
0.45
910
920
0.2 ≤ m/p ≤ 0.3
0.235 ≤ m/p ≤ 0.265

FIG. 9

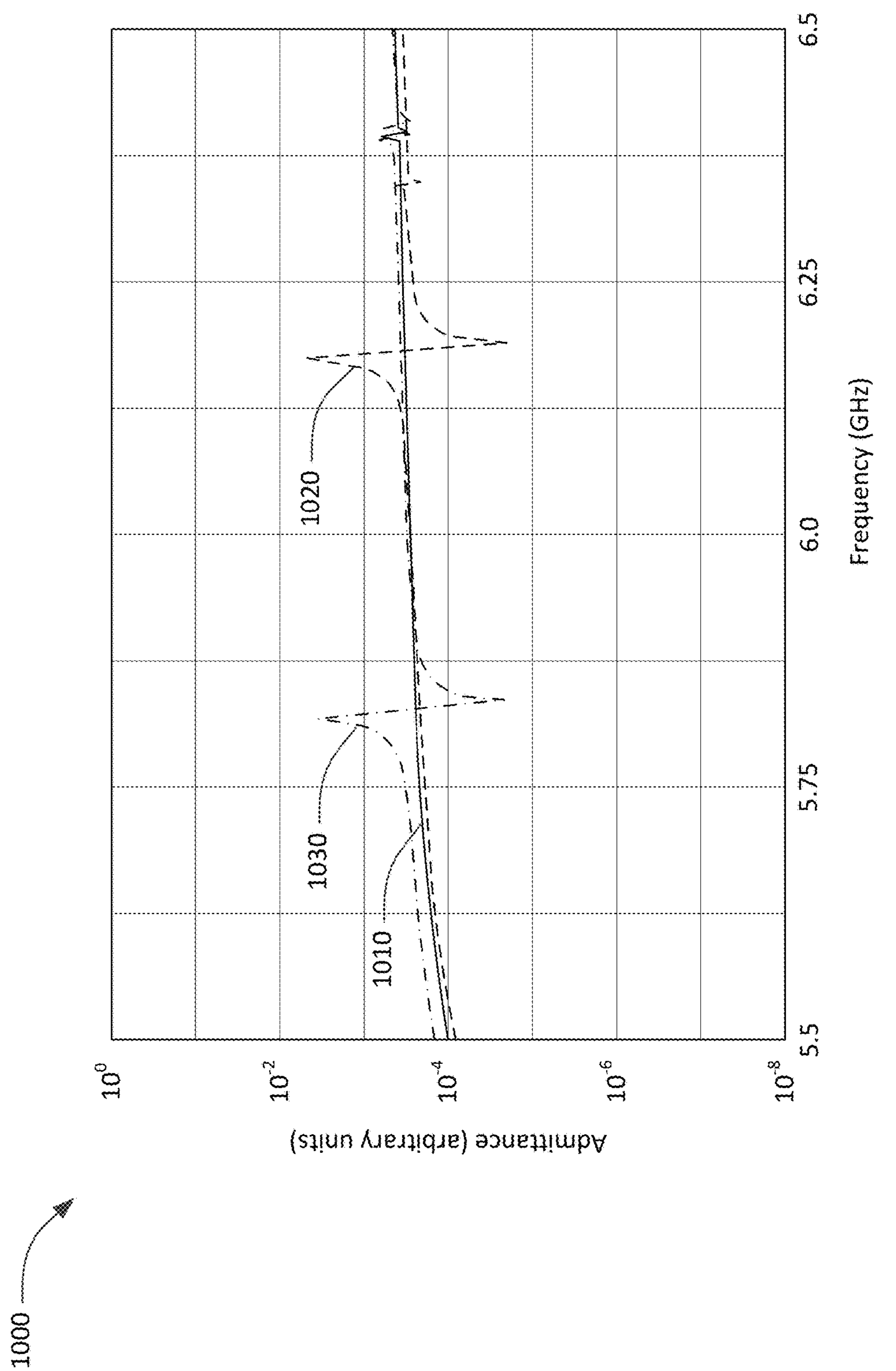
1000
Admittance (arbitrary units)
10^0
10^{-2}
10^{-4}
10^{-6}
10^{-8}
Frequency (GHz)
5.5
5.75
6.0
6.25
6.5
1010
1020
1030

FIG. 10

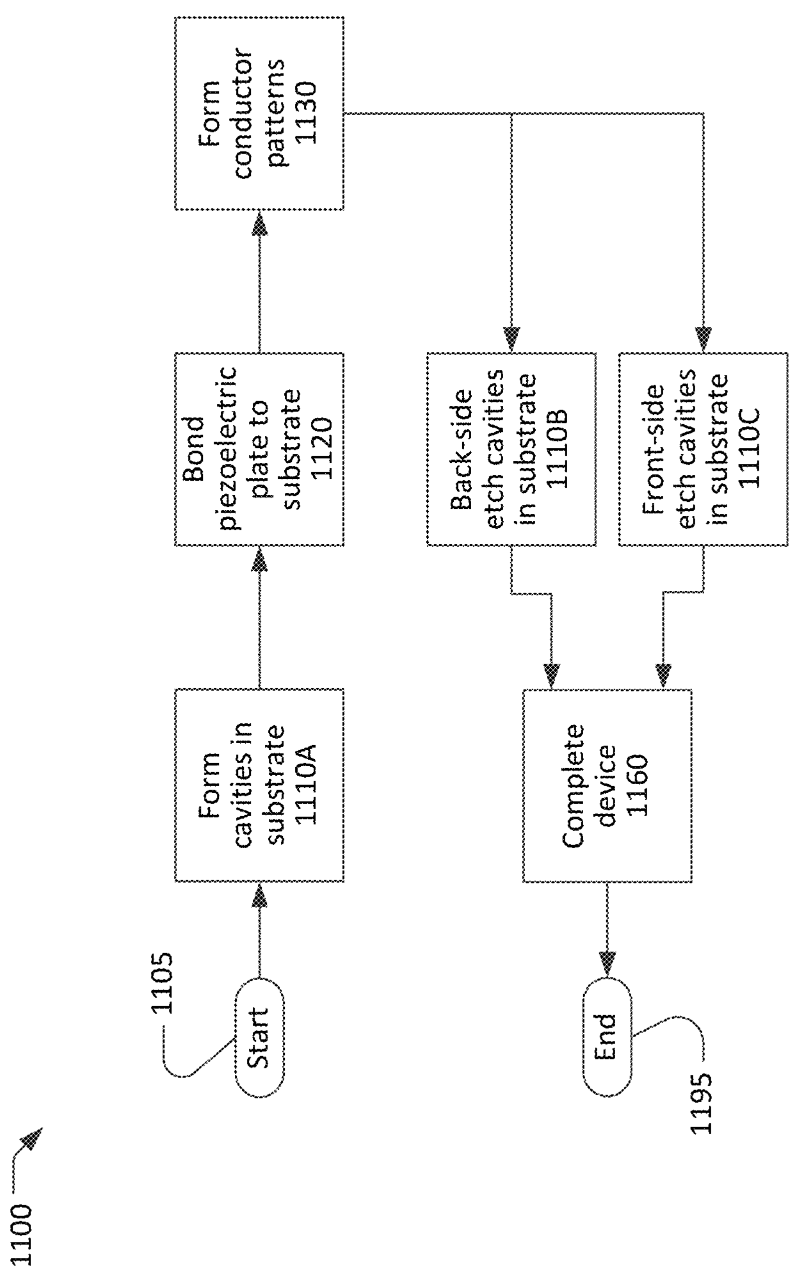

Note: only one of actions 1110A, 1110B, 1110C is performed in each of three variations of the process 1100.

FIG. 11

TRANSVERSELY-EXCITED FILM BULK ACOUSTIC RESONATOR WITH REDUCED SPURIOUS MODES

RELATED APPLICATION INFORMATION

This patent claims priority from provisional patent application 62/904,386, filed Sep. 23, 2019, entitled ANALYSIS OF XBAR RESONANCE AND HIGHER ORDER SPURIOUS MODES.

This patent is also a continuation-in-part of application Ser. No. 16/920,173, filed Jul. 2, 2020, entitled TRANSVERSELY-EXCITED FILM BULK ACOUSTIC RESONATOR, which is a continuation of application Ser. No. 16/438,121, filed Jun. 11, 2019, entitled TRANSVERSELY-EXCITED FILM BULK ACOUSTIC RESONATOR, now U.S. Pat. No. 10,756,697, which is a continuation-in-part of application Ser. No. 16/230,443, filed Dec. 21, 2018, entitled TRANSVERSELY-EXCITED FILM BULK ACOUSTIC RESONATOR, now U.S. Pat. No. 10,491,192 B2, which claims priority from the following provisional patent applications: application 62/685,825, filed Jun. 15, 2018, entitled SHEAR-MODE FBAR (XBAR); application 62/701,363, filed Jul. 20, 2018, entitled SHEAR-MODE FBAR (XBAR); application 62/741,702, filed Oct. 5, 2018, entitled 5 GHZ LATERALLY-EXCITED BULK WAVE RESONATOR (XBAR); application 62/748,883, filed Oct. 22, 2018, entitled SHEAR-MODE FILM BULK ACOUSTIC RESONATOR; and application 62/753,815, filed Oct. 31, 2018, entitled LITHIUM TANTALATE SHEAR-MODE FILM BULK ACOUSTIC RESONATOR. All of these applications are incorporated herein by reference.

NOTICE OF COPYRIGHTS AND TRADE DRESS

BACKGROUND

Field

This disclosure relates to radio frequency filters using acoustic wave resonators, and specifically to filters for use in communications equipment.

Description of the Related Art

A radio frequency (RF) filter is a two-port device configured to pass some frequencies and to stop other frequencies, where "pass" means transmit with relatively low signal loss and "stop" means block or substantially attenuate. The range of frequencies passed by a filter is referred to as the "pass-band" of the filter. The range of frequencies stopped by such a filter is referred to as the "stop-band" of the filter. A typical RF filter has at least one pass-band and at least one stop-band. Specific requirements on a passband or stop-band depend on the specific application. For example, a "pass-band" may be defined as a frequency range where the

insertion loss of a filter is better than a defined value such as 1 dB, 2 dB, or 3 dB. A "stop-band" may be defined as a frequency range where the rejection of a filter is greater than a defined value such as 20 dB, 30 dB, 40 dB, or greater depending on application.

RF filters are used in communications systems where information is transmitted over wireless links. For example, RF filters may be found in the RF front-ends of cellular base stations, mobile telephone and computing devices, satellite transceivers and ground stations, IoT (Internet of Things) devices, laptop computers and tablets, fixed point radio links, and other communications systems. RF filters are also used in radar and electronic and information warfare systems.

RF filters typically require many design trade-offs to achieve, for each specific application, the best compromise between performance parameters such as insertion loss, rejection, isolation, power handling, linearity, size and cost. Specific design and manufacturing methods and enhancements can benefit simultaneously one or several of these requirements.

Performance enhancements to the RF filters in a wireless system can have broad impact to system performance. Improvements in RF filters can be leveraged to provide system performance improvements such as larger cell size, longer battery life, higher data rates, greater network capacity, lower cost, enhanced security, higher reliability, etc. These improvements can be realized at many levels of the wireless system both separately and in combination, for example at the RF module, RF transceiver, mobile or fixed sub-system, or network levels.

The desire for wider communication channel bandwidths will inevitably lead to the use of higher frequency communications bands. The current LTE™ (Long Term Evolution) specification defines frequency bands from 3.3 GHz to 5.9 GHz. These bands are not presently used. Future proposals for wireless communications include millimeter wave communication bands with frequencies up to 28 GHz.

High performance RF filters for present communication systems commonly incorporate acoustic wave resonators including surface acoustic wave (SAW) resonators, bulk acoustic wave (BAW) resonators, film bulk acoustic wave resonators (FBAR), and other types of acoustic resonators. However, these existing technologies are not well-suited for use at the higher frequencies proposed for future communications networks.

DESCRIPTION OF THE DRAWINGS

FIG. **1** has a schematic plan view and two schematic cross-sectional views of a transversely-excited film bulk acoustic resonator (XBAR).

FIG. **2** is an expanded schematic cross-sectional view of a portion of the XBAR of FIG. **1**.

FIG. **3** is an alternative schematic cross-sectional view of the XBAR of FIG. **1**.

FIG. **4** is a graphic illustrating a shear primary acoustic mode in an XBAR.

FIG. **5** is a schematic block diagram of a filter using XBARs.

FIG. **6** is a graph of the magnitude of admittance versus frequency for an XBAR.

FIG. **7** is a graph of the frequency and coupling of a primary shear mode and the frequency of an A1-3 spurious mode as functions of interdigital transducer (IDT) pitch.

FIG. **8** is a graph of the frequency and coupling of the A1-3 spurious mode as functions of IDT mark-to-pitch ratio.

FIG. **9** is a graph of absolute admittance and frequency of the A1-3 spurious mode as functions of IDT mark-to-pitch ratio.

FIG. **10** is a graph of the magnitude of admittance versus frequency for three XBARs with different mark-to-pitch ratios.

FIG. **11** is a flow chart of a process for fabricating an XBAR or filter incorporating XBARs.

Throughout this description, elements appearing in figures are assigned three-digit or four-digit reference designators, where the two least significant digits are specific to the element and the one or two most significant digit is the figure number where the element is first introduced. An element that is not described in conjunction with a figure may be presumed to have the same characteristics and function as a previously-described element having the same reference designator.

DETAILED DESCRIPTION

Description of Apparatus

FIG. **1** shows a simplified schematic top view and orthogonal cross-sectional views of a transversely-excited film bulk acoustic resonator (XBAR) **100**. XBAR resonators such as the resonator **100** may be used in a variety of RF filters including band-reject filters, band-pass filters, duplexers, and multiplexers. XBARs are well suited for use in filters for communications bands with frequencies above 3 GHz.

The XBAR **100** is made up of a thin film conductor pattern formed on a surface of a piezoelectric plate **110** having a front surface **112** and a back surface **114**. The front and back surfaces are essentially parallel. "Essentially parallel" means parallel to the extent possible within normal manufacturing tolerances. The piezoelectric plate is a thin single-crystal layer of a piezoelectric material such as lithium niobate, lithium tantalate, lanthanum gallium silicate, gallium nitride, or aluminum nitride. The piezoelectric plate is cut such that the orientation of the X, Y, and Z crystalline axes with respect to the front and back surfaces is known and consistent. In the examples presented in this patent, the piezoelectric plates are Z-cut, which is to say the Z axis is normal to the front surface **112** and back surface **114**. However, XBARs may be fabricated on piezoelectric plates with other crystallographic orientations including rotated Z-cut and rotated YX-cut.

The back surface **114** of the piezoelectric plate **110** is attached to a surface **122** of the substrate **120** except for a portion of the piezoelectric plate **110** that forms a diaphragm **115** spanning a cavity **140** formed in the substrate **120**. The cavity **140** has a perimeter defined by the intersection of the cavity and the surface **122** of the substrate **120**. The portion of the piezoelectric plate that spans the cavity is referred to herein as the "diaphragm" due to its physical resemblance to the diaphragm of a microphone. As shown in FIG. **1**, the diaphragm **115** is contiguous with the rest of the piezoelectric plate **110** around all of the perimeter **145** of the cavity **140**. In this context, "contiguous" means "continuously connected without any intervening item".

The substrate **120** provides mechanical support to the piezoelectric plate **110**. The substrate **120** may be, for example, silicon, sapphire, quartz, or some other material or combination of materials. The back surface **114** of the piezoelectric plate **110** may be attached to the substrate **120** using a wafer bonding process. Alternatively, the piezoelectric plate **110** may be grown on the substrate **120** or otherwise attached to the substrate. The piezoelectric plate **110** may be attached directly to the substrate or may be attached to the substrate **120** via one or more intermediate material layers.

The cavity **140** is an empty space within a solid body of the resonator **100**. The cavity **140** may be a hole completely through the substrate **120** (as shown in Section A-A and Section B-B) or a recess in the substrate **120** (as shown subsequently in FIG. **3**). The cavity **140** may be formed, for example, by selective etching of the substrate **120** before or after the piezoelectric plate **110** and the substrate **120** are attached.

The conductor pattern of the XBAR **100** includes an interdigital transducer (IDT) **130**. An IDT is an electrode structure for converting between electrical and acoustic energy in piezoelectric devices. The IDT **130** includes a first plurality of parallel elongated conductors, commonly called "fingers", such as finger **136**, extending from a first busbar **132**. The IDT **130** includes a second plurality of fingers extending from a second busbar **134**. The first and second pluralities of parallel fingers are interleaved. The interleaved fingers overlap for a distance AP, commonly referred to as the "aperture" of the IDT. The center-to-center distance L between the outermost fingers of the IDT **130** is the "length" of the IDT.

The term "busbar" refers to the conductors that interconnect the first and second sets of fingers in an IDT. As shown in FIG. **1**, each busbar **132**, **134** is an elongated rectangular conductor with a long axis orthogonal to the interleaved fingers and having a length approximately equal to the length L of the IDT. The busbars of an IDT need not be rectangular or orthogonal to the interleaved fingers and may have lengths longer than the length of the IDT.

The first and second busbars **132**, **134** serve as the terminals of the XBAR **100**. A radio frequency or microwave signal applied between the two busbars **132**, **134** of the IDT **130** excites a primary acoustic mode within the piezoelectric plate **110**. As will be discussed in further detail, the primary acoustic mode is a bulk shear mode where acoustic energy propagates along a direction substantially orthogonal to the surface of the piezoelectric plate **110**, which is also normal, or transverse, to the direction of the electric field created by the IDT fingers. Thus, the XBAR is considered a transversely-excited film bulk wave resonator.

The IDT **130** is positioned on the piezoelectric plate **110** such that at least the fingers of the IDT **130** are disposed on the diaphragm **115** of the piezoelectric plate that spans, or is suspended over, the cavity **140**. As shown in FIG. **1**, the cavity **140** has a rectangular shape with an extent greater than the aperture AP and length L of the IDT **130**. A cavity of an XBAR may have a different shape, such as a regular or irregular polygon. The cavity of an XBAR may more or fewer than four sides, which may be straight or curved.

For ease of presentation in FIG. **1**, the geometric pitch and width of the IDT fingers is greatly exaggerated with respect to the length (dimension L) and aperture (dimension AP) of the XBAR. An XBAR for a 5G device will have more than ten parallel fingers in the IDT **110**. An XBAR may have hundreds, possibly thousands, of parallel fingers in the IDT **110**. Similarly, the thickness of the fingers in the cross-sectional views is greatly exaggerated in the drawings.

FIG. **2** shows a detailed schematic cross-sectional view of the XBAR **100**. The piezoelectric plate **110** is a single-crystal layer of piezoelectrical material having a thickness ts. ts may be, for example, 100 nm to 1500 nm. When used in filters for LTE™ bands from 3.4 GHZ to 6 GHz (e.g. bands 42, 43, 46), the thickness ts may be, for example, 200 nm to 1000 nm.

A front-side dielectric layer **214** may be formed on the front side of the piezoelectric plate **110**. The "front side" of the XBAR is the surface facing away from the substrate. The front-side dielectric layer **214** has a thickness tfd. The front-side dielectric layer **214** is formed between the IDT fingers **238**. Although not shown in FIG. **2**, the front side dielectric layer **214** may also be deposited over the IDT fingers **238**. A back-side dielectric layer **216** may be formed on the back side of the piezoelectric plate **110**. The back-side dielectric layer **216** has a thickness tbd. The front-side and back-side dielectric layers **214**, **216** may be a non-piezoelectric dielectric material, such as silicon dioxide or silicon nitride. tfd and tbd may be, for example, 0 to 500 nm. tfd and tbd are typically less than the thickness ts of the piezoelectric plate. tfd and tbd are not necessarily equal, and the front-side and back-side dielectric layers **214**, **216** are not necessarily the same material. Either or both of the front-side and back-side dielectric layers **214**, **216** may be formed of multiple layers of two or more materials.

The IDT fingers **238** may be one or more layers of aluminum, a substantially aluminum alloys, copper, a substantially copper alloys, beryllium, gold, molybdenum, or some other conductive material. Thin (relative to the total thickness of the conductors) layers of other metals, such as chromium or titanium, may be formed under and/or over the fingers to improve adhesion between the fingers and the piezoelectric plate **110** and/or to passivate or encapsulate the fingers. The busbars (**132**, **134** in FIG. **1**) of the IDT may be made of the same or different materials as the fingers. As shown in FIG. **2**, the IDT fingers **238** have rectangular cross-sections. The IDT fingers may have some other cross-sectional shape, such as trapezoidal.

Dimension p is the center-to-center spacing or "pitch" of the IDT fingers, which may be referred to as the pitch of the IDT and/or the pitch of the XBAR. Dimension w is the width or "mark" of the IDT fingers. The IDT of an XBAR differs substantially from the IDTs used in surface acoustic wave (SAW) resonators. In a SAW resonator, the pitch of the IDT is one-half of the acoustic wavelength at the resonance frequency. Additionally, the mark-to-pitch ratio of a SAW resonator IDT is typically close to 0.5 (i.e., the mark or finger width is about one-fourth of the acoustic wavelength at resonance). In an XBAR, the pitch p of the IDT is typically 2 to 20 times the width w of the fingers. In addition, the pitch p of the IDT is typically 2 to 20 times the thickness ts of the piezoelectric slab **212**. The width of the IDT fingers in an XBAR is not constrained to one-fourth of the acoustic wavelength at resonance. For example, the width of XBAR IDT fingers may be 500 nm or greater, such that the IDT can be fabricated using optical lithography. The thickness tm of the IDT fingers may be from 100 nm to about equal to the width w. The thickness of the busbars (**132**, **134** in FIG. **1**) of the IDT may be the same as, or greater than, the thickness tm of the IDT fingers.

FIG. **3** is a plan view and a cross-sectional view of another XBAR **300** which is similar to the XBAR **100** of FIG. **1**. A piezoelectric plate **310** is attached to a substrate **320**. A portion of the piezoelectric plate **310** forms a diaphragm **315** spanning a cavity **340** in the substrate **320**. An IDT **330** is formed on the surface **312** of the piezoelectric plate as previously described.

Unlike the cavity **140** of FIG. **1**, the cavity **340** does not fully penetrate the substrate **320**. The cavity **340** may be formed, for example, by etching the substrate **320** before attaching the piezoelectric plate **310**. Alternatively, the cavity **340** may be formed by etching the substrate **320** with a selective etchant that reaches the substrate through one or more openings, such as opening **350**, provided in the piezoelectric plate **310**. In this case, the diaphragm **315** may be contiguous with the rest of the piezoelectric plate **310** around a large portion of a perimeter **345** of the cavity **340**. For example, the diaphragm **315** may be contiguous with the rest of the piezoelectric plate **310** around at least 50% of the perimeter **345** of the cavity **340**.

FIG. **4** is a graphical illustration of the primary acoustic mode of interest in an XBAR. FIG. **4** shows a small portion of an XBAR **400** including a piezoelectric plate **410** and three interleaved IDT fingers **430**. A radio frequency (RF) voltage is applied to the interleaved fingers **430**. This voltage creates a time-varying electric field between the fingers. The direction of the electric field is primarily lateral, or parallel to the surface of the piezoelectric plate **410**, as indicated by the arrows labeled "electric field". Since the dielectric constant of the piezoelectric plate is significantly higher than the surrounding air, the electric field is highly concentrated in the plate relative to the air. The lateral electric field introduces shear deformation, and thus strongly excites a shear-mode acoustic mode, in the piezoelectric plate **410**. Shear deformation is deformation in which parallel planes in a material remain parallel and maintain a constant distance while translating relative to each other. A "shear acoustic mode" is an acoustic vibration mode in a medium that results in shear deformation of the medium. The shear deformations in the XBAR **400** are represented by the curves **460**, with the adjacent small arrows providing a schematic indication of the direction and magnitude of atomic motion. The degree of atomic motion, as well as the thickness of the piezoelectric plate **410**, have been greatly exaggerated for ease of visualization. While the atomic motions are predominantly lateral (i.e. horizontal as shown in FIG. **4**), the direction of acoustic energy flow of the excited primary shear acoustic mode is substantially orthogonal to the surface of the piezoelectric plate, as indicated by the arrow **465**.

An acoustic resonator based on shear acoustic wave resonances can achieve better performance than current state-of-the art film-bulk-acoustic-resonators (FBAR) and solidly-mounted-resonator bulk-acoustic-wave (SMR BAW) devices where the electric field is applied in the thickness direction. In such devices, the acoustic mode is compressive with atomic motions and the direction of acoustic energy flow in the thickness direction. In addition, the piezoelectric coupling for shear wave XBAR resonances can be high (>20%) compared to other acoustic resonators. High piezoelectric coupling enables the design and implementation of microwave and millimeter-wave filters with appreciable bandwidth.

FIG. **5** is a schematic circuit diagram and layout for a high frequency band-pass filter **500** using XBARs. The filter **500** has a conventional ladder filter architecture including three series resonators **510**A, **510**B, **510**C and two shunt resonators **520**A, **520**B. The three series resonators **510**A, **510**B, and **510**C are connected in series between a first port and a second port (hence the term "series resonator"). In FIG. **5**, the first and second ports are labeled "In" and "Out", respectively. However, the filter **500** is bidirectional and either port may serve as the input or output of the filter. The two shunt resonators **520**A, **520**B are connected from nodes between the series resonators to ground. A filter may contain additional reactive components, such as inductors, not shown in FIG. **5**. All the shunt resonators and series resonators are XBARs. The inclusion of three series and two shunt resonators is exemplary. A filter may have more or fewer than five total resonators, more or fewer than three series resonators, and more or fewer than two shunt resonators. Typically, all of the series resonators are connected in series between an input and an output of the filter. All of the shunt resonators are typically connected between ground and the input, the output, or a node between two series resonators.

In the exemplary filter **500**, the three series resonators **510**A, B, C and the two shunt resonators **520**A, B of the filter **500** are formed on a single plate **530** of piezoelectric material bonded to a silicon substrate (not visible). Each resonator includes a respective IDT (not shown), with at least the fingers of the IDT disposed over a cavity in the substrate. In this and similar contexts, the term "respective" means "relating things each to each", which is to say with a one-to-one correspondence. In FIG. **5**, the cavities are illustrated schematically as the dashed rectangles (such as the rectangle **535**). In this example, each IDT is disposed over a respective cavity. In other filters, the IDTs of two or more resonators may be disposed over a single cavity.

Each of the resonators **510**A, **510**B, **510**C, **520**A, **520**B in the filter **500** has resonance where the admittance of the resonator is very high and an anti-resonance where the admittance of the resonator is very low. The resonance and anti-resonance occur at a resonance frequency and an anti-resonance frequency, respectively, which may be the same or different for the various resonators in the filter **500**. In over-simplified terms, each resonator can be considered a short-circuit at its resonance frequency and an open circuit at its anti-resonance frequency. The input-output transfer function will be near zero at the resonance frequencies of the shunt resonators and at the anti-resonance frequencies of the series resonators. In a typical filter, the resonance frequencies of the shunt resonators are positioned below the lower edge of the filter's passband and the anti-resonance frequencies of the series resonators are positioned above the upper edge of the passband.

FIG. **6** is a graph **600** of the performance of a typical XBAR. The curve **610** is a plot of the magnitude of the admittance of an XBAR device having a lithium niobate diaphragm. The diaphragm thickness is 400 nm. The IDT conductors are aluminum, 100 nm thick. The IDT pitch is 3 μm and the IDT mark or finger width is 500 nm. The primary shear acoustic mode has a resonance **620** at a frequency of 4.8 GHz and an anti-resonance **625** at a frequency about 5.4 GHz. The coupling of the primary mode is greater than 25% and the Q at the resonance and anti-resonance frequencies is 400 to 500.

The solid curve **610** also exhibits multiple spurious modes. The largest spurious mode is an A1-3 mode (the third harmonic of the primary shear acoustic mode) with a resonance **630** and anti-resonance **635** at about 6.25 GHz. Small spurious modes **640** are high order harmonics of plate wave modes that travel along the length of the XBAR in a direction normal to the IDT fingers. Data presented in FIG. **6** and subsequent figures is derived from two-dimensional simulation of XBARs using a finite-element technique.

FIG. **7** is a graph **700** of relationships between XBAR performance and IDT pitch. The solid curve **710** is a plot of the resonance frequency of the XBAR shear primary mode as a function of IDT pitch for an XBAR with a z-cut lithium niobate diaphragm 400 nm thick and aluminum conductors 100 nm thick. The diaphragm thickness is the dominant parameter that determines resonance frequency of an XBAR. The resonance frequency has a smaller dependence on IDT pitch. As shown in FIG. **7**, varying the IDT pitch from 1 μm to 6 μm results in reduction in resonance frequency by about 25%.

The dashed curve **720** is a plot of the resonance frequency of the A1-3 spurious mode of the same XBAR as a function of IDT pitch. Diaphragm thickness is also the dominant parameter that determines resonance frequency of A1-3 mode. However, the resonance frequency of the A1-3 mode has a much larger dependence on IDT pitch compared to the shear primary mode. Varying the IDT pitch from 1 μm to 6 μm results in reduction in resonance frequency of the A1-4 mode by about 85%. The frequencies of other spurious modes (i.e. spurious modes **640** in FIG. **6**) are also very dependent on IDT pitch.

The dot-dash curve **730** is a plot of electromechanical coupling of the shear primary mode as a function of IDT pitch. The relationship between coupling and pitch is nonlinear. Larger IDT pitch results in higher coupling and coupling decreases rapidly for pitch values less than 3 μm. However, 17% coupling is available at pitch value of 1 μm, which is still sufficient for many filter applications.

FIG. **8** is a graph **800** of relationships between XBAR performance and IDT mark-to-pitch ratio (mark/pitch). The solid curve **810** is a plot of the resonance frequency of the XBAR shear primary mode as a function of IDT mark/pitch for an XBAR with a z-cut lithium niobate diaphragm 400 nm thick. The IDT conductors are aluminum 100 nm thick and the IDT pitch is 3 μm. The diaphragm thickness is the dominant parameter that determines resonance frequency of an XBAR. The resonance frequency has a smaller dependence on IDT mark/pitch. As shown in FIG. **8**, varying the IDT mark/pitch from 0.15 to 0.45 μm results in reduction in resonance frequency by about 6%.

The dashed curve **820** is a plot of electromechanical coupling of the shear primary mode as a function of IDT mark/pitch. The relationship between coupling and mark/pitch is nonlinear. Maximum coupling occurs for IDT mark/pitch between 0.40 and 0.45. Coupling decreases with decreasing mark/pitch. However, 27% coupling is available at mark/pitch value of about 0.12, which is sufficient for most filter applications.

FIG. **7** and FIG. **8** illustrate the complexity of selecting the pitch and mark of XBAR IDTs within a filter to provide a desired resonance frequency and electromechanical coupling of each XBAR while trying to place spurious modes at frequencies that do not degrade the filter performance. In particular, since the resonance frequency of the shear primary acoustic mode varies with both IDT pitch and IDT mark, the pitch and mark must be selected in combination to set the resonance frequency of an XBAR to a predetermined target frequency. Since the same resonance frequency may be achieved with different IDT pitch and mark combinations, a filter designer has some freedom to select the pitch and mark to control the frequencies of spurious modes.

FIG. **9** is a graph **900** of relationships between the A1-3 spurious mode and IDT mark-to-pitch ratio (mark/pitch). The solid curve **910** is a plot of the resonance frequency of the A1-3 mode as a function of IDT mark/pitch for an XBAR with a z-cut lithium niobate diaphragm 400 nm thick. The IDT conductors are aluminum 100 nm thick and the IDT pitch is 3 μm. The A1-3 mode resonance frequency depends on IDT mark/pitch. As shown in FIG. **9**, varying the IDT mark/pitch from 0.15 to 0.45 μm results in reduction in resonance frequency by about 10%.

The dashed curve **920** is a plot of the absolute admittance of the A1-3 mode as a function of IDT mark/pitch. The relationship between admittance and mark/pitch is nonlinear. Minimum admittance occurs for IDT mark/pitch from

0.235 to 0.265. Admittance increase for mark/pitch values outside of this range but is still small for a mark/pitch range from 0.2 to 0.3.

FIG. **10** is a graph **1000** of the performance of three XBARs having different mark/pitch ratios. Specifically, the solid line **1010** is a plot of the magnitude of admittance of an XBAR with m/p=0.25. The dashed line **1020** is a plot of the magnitude of admittance of an XBAR with m/p=0.2. The dot-dash line **1030** is a plot of the magnitude of admittance of an XBAR with m/p=0.3. All three XBARs have z-cut lithium niobate diaphragms 400 nm thick. The IDT conductors are aluminum 100 nm thick and the IDT pitch is 3 μm. An A1-3 mode is present for the XBARs with m/p=0.2 and m/p=0.3. The A1-3 mode is not present in the XBAR with m/p=0.25 (solid line **1010**).

FIG. **9** and FIG. **10** demonstrate that selecting IDT mark/pitch in a range from 0.2 to 0.3, or in a preferred range of 0.235 to 0.265, reduces or eliminates the A1-3 spurious mode. It is anticipated that this range will be valid for values of IDT pitch greater than or less than 3 μm and for thin aluminum IDT conductors with a thickness between 50 nm and 150 nm.

Description of Methods

FIG. **11** is a simplified flow chart showing a process **1100** for making an XBAR or a filter incorporating XBARs. The process **1100** starts at **1105** with a substrate and a plate of piezoelectric material and ends at **1195** with a completed XBAR or filter. The flow chart of FIG. **11** includes only major process steps. Various conventional process steps (e.g. surface preparation, cleaning, inspection, baking, annealing, monitoring, testing, etc.) may be performed before, between, after, and during the steps shown in FIG. **11**.

The flow chart of FIG. **11** captures three variations of the process **1100** for making an XBAR which differ in when and how cavities are formed in the substrate. The cavities may be formed at steps **1110**A, **1110**B, or **1110**C. Only one of these steps is performed in each of the three variations of the process **1100**.

The piezoelectric plate may be, for example, Z-cut lithium niobate as used in the previously presented examples. The piezoelectric plate may be rotated ZY-lithium niobate or rotated YX-cut lithium niobate. The piezoelectric plate may be some other material and/or some other cut. The substrate may preferably be silicon. The substrate may be some other material that allows formation of deep cavities by etching or other processing.

In one variation of the process **1100**, one or more cavities are formed in the substrate at **1110**A before the piezoelectric plate is bonded to the substrate at **1120**. A separate cavity may be formed for each resonator in a filter device. The one or more cavities may be formed using conventional photolithographic and etching techniques. Typically, the cavities formed at **1110**A will not penetrate through the substrate, and the resulting resonator devices will have a cross-section as shown in FIG. **3**.

At **1120**, the piezoelectric plate is bonded to the substrate. The piezoelectric plate and the substrate may be bonded by a wafer bonding process. Typically, the mating surfaces of the substrate and the piezoelectric plate are highly polished. One or more layers of intermediate materials, such as an oxide or metal, may be formed or deposited on the mating surface of one or both of the piezoelectric plate and the substrate. One or both mating surfaces may be activated using, for example, a plasma process. The mating surfaces may then be pressed together with considerable force to establish molecular bonds between the piezoelectric plate and the substrate or intermediate material layers.

A conductor pattern, including IDTs of each XBAR, is formed at **1130** by depositing and patterning one or more conductor layers on the front side of the piezoelectric plate. The conductor layer may be, for example, aluminum or an aluminum alloy with a thickness of 50 nm to 150 nm. Optionally, one or more layers of other materials may be disposed below (i.e. between the conductor layer and the piezoelectric plate) and/or on top of the conductor layer. For example, a thin film of titanium, chrome, or other metal may be used to improve the adhesion between the conductor layer and the piezoelectric plate. A conduction enhancement layer of gold, aluminum, copper or other higher conductivity metal may be formed over portions of the conductor pattern (for example the IDT bus bars and interconnections between the IDTs).

The conductor pattern may be formed at **1130** by depositing the conductor layer and, optionally, one or more other metal layers in sequence over the surface of the piezoelectric plate. The excess metal may then be removed by etching through patterned photoresist. The conductor layer can be etched, for example, by plasma etching, reactive ion etching, wet chemical etching, and other etching techniques.

Alternatively, the conductor pattern may be formed at **1130** using a lift-off process. Photoresist may be deposited over the piezoelectric plate. and patterned to define the conductor pattern. The conductor layer and, optionally, one or more other layers may be deposited in sequence over the surface of the piezoelectric plate. The photoresist may then be removed, which removes the excess material, leaving the conductor pattern.

In a second variation of the process **1100**, one or more cavities are formed in the back side of the substrate at **1110**B. A separate cavity may be formed for each resonator in a filter device. The one or more cavities may be formed using an anisotropic or orientation-dependent dry or wet etch to open holes through the back side of the substrate to the piezoelectric plate. In this case, the resulting resonator devices will have a cross-section as shown in FIG. **1**.

In a third variation of the process **1100**, one or more cavities in the form of recesses in the substrate may be formed at **1110**C by etching the substrate using an etchant introduced through openings in the piezoelectric plate. A separate cavity may be formed for each resonator in a filter device. The one or more cavities formed at **1110**C will not penetrate through the substrate, and the resulting resonator devices will have a cross-section as shown in FIG. **3**.

In all variations of the process **1100**, the filter device is completed at **1160**. Actions that may occur at **1160** include depositing a passivation and tuning layer such as SiO_2 or Si_3O_4 over all or a portion of the device; forming bonding pads or solder bumps or other means for making connection between the device and external circuitry; excising individual devices from a wafer containing multiple devices; other packaging steps; and testing. Any dielectric layer deposited at **1160** or elsewhere in the process **1100** is deposited over all resonators. Another action that may occur at **1160** is to tune the resonant frequencies of the resonators within the device by adding or removing metal or dielectric material from the front side of the device. After the filter device is completed, the process ends at **1195**.

Closing Comments

Throughout this description, the embodiments and examples shown should be considered as exemplars, rather than limitations on the apparatus and procedures disclosed or claimed. Although many of the examples presented herein involve specific combinations of method acts or system elements, it should be understood that those acts and those elements may be combined in other ways to accomplish the same objectives. With regard to flowcharts, additional and fewer steps may be taken, and the steps as shown may be combined or further refined to achieve the methods described herein. Acts, elements and features discussed only in connection with one embodiment are not intended to be excluded from a similar role in other embodiments.

As used herein, "plurality" means two or more. As used herein, a "set" of items may include one or more of such items. As used herein, whether in the written description or the claims, the terms "comprising", "including", "carrying", "having", "containing", "involving", and the like are to be understood to be open-ended, i.e., to mean including but not limited to. Only the transitional phrases "consisting of" and "consisting essentially of", respectively, are closed or semi-closed transitional phrases with respect to claims. Use of ordinal terms such as "first", "second", "third", etc., in the claims to modify a claim element does not by itself connote any priority, precedence, or order of one claim element over another or the temporal order in which acts of a method are performed, but are used merely as labels to distinguish one claim element having a certain name from another element having a same name (but for use of the ordinal term) to distinguish the claim elements. As used herein, "and/or" means that the listed items are alternatives, but the alternatives also include any combination of the listed items.

It is claimed:

1. An acoustic resonator device comprising:

a substrate having a surface;

a single-crystal piezoelectric plate having front and back surfaces, the back surface attached to the surface of the substrate except for a portion of the piezoelectric plate forming a diaphragm that spans a cavity in the substrate; and

a conductor pattern formed on the front surface of the piezoelectric plate, the conductor pattern including an interdigital transducer (IDTs), interleaved fingers of the IDT disposed on the diaphragm,

wherein a pitch of the interleaved fingers and a mark of the interleaved fingers are set in combination such that a resonance frequency of the acoustic resonator is equal to a predetermined target frequency, and

a ratio of the mark of the interleaved fingers to the pitch of the interleaved fingers is greater than or equal to 0.2 and less than or equal to 0.3.

2. The device of claim **1**, wherein

a ratio of the mark of the interleaved fingers to the pitch of the interleaved fingers is greater than or equal to 0.235 and less than or equal to 0.265.

3. The device of claim **1**, wherein the diaphragm is contiguous with the piezoelectric plate around at least 50% of a perimeter of the cavity.

4. The device of claim **1** wherein the interleaved fingers of the IDT are aluminum with a thickness greater than or equal to 50 nm and less than or equal to 150 nm.

5. The device of claim **1**, wherein the single-crystal piezoelectric plate and the IDT are configured such that a radio frequency signal applied to the IDT excites a shear primary acoustic mode within the diaphragm.

6. The device of claim **1**, wherein the single-crystal piezoelectric plate is lithium niobate.

7. An acoustic filter device comprising:

a substrate having a surface;

a single-crystal piezoelectric plate having front and back surfaces, the back surface attached to the surface of the substrate except for portions of the piezoelectric plate forming a plurality of diaphragms spanning respective cavities in the substrate; and

a conductor pattern formed on the front surface of the piezoelectric plate, the conductor pattern including interdigital transducers (IDTs) of a plurality of acoustic resonators, interleaved fingers of each IDT disposed on a respective diaphragm from the plurality of diaphragms,

wherein, for each of the IDTs, a pitch of the interleaved fingers and a mark of the interleaved fingers are set in combination such that a resonance frequency of the respective acoustic resonator is equal to a respective predetermined target frequency, and

for one or more of the IDTs, a ratio of the mark of the interleaved fingers to the pitch of the interleaved fingers is greater than or equal to 0.2 and less than or equal to 0.3.

8. The device of claim **7**, wherein

for one or more of the IDTs, a ratio of the mark of the interleaved fingers to the pitch of the interleaved fingers is greater than or equal to 0.235 and less than or equal to 0.265.

9. The device of claim **7**, wherein the single-crystal piezoelectric plate is lithium niobate.

10. The device of claim **7**, wherein each of the plurality of diaphragms is contiguous with the piezoelectric plate around at least 50% of a perimeter of the cavity.

11. The device of claim **7** wherein the interleaved fingers of all of the IDTs are aluminum with a thickness greater than or equal to 50 nm and less than or equal to 150 nm.

12. The device of claim **7**, wherein the single-crystal piezoelectric plate and the plurality of IDTs are configured such that respective radio frequency signals applied to the plurality of IDTs excite respective shear primary acoustic modes within the respective diaphragms.

13. A method of fabricating an acoustic resonator device, comprising:

bonding a back surface of a single-crystal piezoelectric plate to a surface of a substrate, a portion of the piezoelectric plate forming a diaphragm that spans a cavity in the substrate; and

forming a conductor pattern on a front surf ace of the piezoelectric plate, the conductor pattern comprising an interdigital transducers (IDT), interleaved fingers of the IDT disposed on the diaphragm; and

wherein a pitch of the interleaved fingers and a mark of the interleaved fingers are set in combination such that a resonance frequency of the acoustic resonator is equal to a predetermined target frequency, and

a ratio of the mark of the interleaved fingers to the pitch of the interleaved fingers is greater than or equal to 0.2 and less than or equal to 0.3.

14. The method of claim **13**, wherein

a ratio of the mark of the interleaved fingers to the pitch of the interleaved fingers is greater than or equal to 0.235 and less than or equal to 0.265.

15. The method of claim **13**, wherein the single-crystal piezoelectric plate and the IDT are configured such that a radio frequency signal applied to the IDT excites a shear primary acoustic mode within the diaphragm.

16. The method of claim **13**, wherein the single-crystal piezoelectric plate is lithium niobate.

17. The method of claim **13**, wherein the diaphragm is contiguous with the piezoelectric plate around at least 50% of a perimeter of the cavity.

18. The method of claim **13**, wherein the interleaved fingers of the IDT are aluminum with a thickness greater than or equal to 50 nm and less than or equal to 150 nm.

* * * * *